Indonesian Journal of Maritime Technology (ISMATECH)

Vol. 03, Issue 02, December 2025

eISSN: 3025-518X

DOI: https://doi.org/10.35718/ ismatech.v3i1. 8481529



Fatigue Life Analysis of Subsea Pipelines due to Vortex Induced Vibration (Viv) at Free Span Case: Wnts (West Natuna Transportation System)

Hifzul Anwar Siregar¹, Luh Putri Adnyani^{1*}, Samsu Dlukha Nurcholik², Destyariani Liana Putri¹

KEYWORDS

Free Span, Vortex-Induced Vibration (VIV), Heading Flow, Fatigue, DNV-RP-F105 **ABSTRACT** – Subsea pipelines in free-span conditions are highly susceptible to Vortex-Induced Vibration (VIV), which generates cyclic stresses and accelerates fatigue failure. This study investigates the fatigue life of a West Natuna Transportation System (WNTS) subsea pipeline under varying heading flow angles (30°, 45°, and 90°) using ANSYS CFD simulations and the Palmgren-Miner fatigue model, in accordance with DNV-RP-F105. Simulations considered Reynolds numbers of 100, 500, and 3.91×10⁵ to capture laminar-to-turbulent flow regimes. Results show that the 90° heading flow produces the most severe VIV, with maximum bending stresses up to 5.59×10⁸ Pa and a corresponding minimum fatigue life of less than 10⁵ cycles, while 30° heading yields significantly longer lifespans, exceeding 10¹⁶ cycles in some cases. Average fatigue life decreased by up to 99.99% when flow incidence increased from 30° to 90° under turbulent conditions. The findings highlight that pipeline orientation relative to prevailing currents strongly influences vortex dynamics, and that aligning pipelines at oblique angles (30° – 45°) can substantially reduce fatigue damage risk. These insights can inform the design and operational strategies of subsea pipeline systems in regions with strong and variable currents, such as the Natuna Sea.

INTRODUCTION

Subsea pipelines play a crucial role in transporting hydrocarbons from offshore production sites to onshore processing facilities or export terminals. These infrastructures are often subjected to harsh subsea environments, including strong currents, irregular seabed, and sediment transport processes, which can compromise structural stability. One of the major challenges in subsea pipeline design and maintenance is the free span phenomenon, where sections of the pipeline become unsupported due to seabed irregularities. This condition can result in dynamic loading from currents and waves, potentially leading to structural failure if not properly assessed [1-3]. A critical factor affecting pipelines in free span conditions is Vortex-Induced Vibration (VIV). VIV occurs when alternating vortex shedding creates oscillatory lift forces that can cause cyclic stress on the pipeline. Over time, these oscillations contribute to material fatigue, which significantly reduces the pipeline's service life [4, 5]. The effect becomes more critical when the vortex shedding frequency approaches the natural frequency of the pipeline, resulting in resonance and increased amplitude of vibration [6].

Recent advancements in numerical modeling, especially Computational Fluid Dynamics (CFD), have enabled better simulation and understanding of fluid–structure interactions in subsea conditions. CFD simulations provide insights into how heading flow angles affect flow separation, pressure distribution, and hydrodynamic forces around pipelines [7-11]. Flow incidence angles such as 30° , 45° , and 90° can significantly alter vortex patterns and increase fatigue risks depending on the interaction of the flow with the pipeline's geometry.

The West Natuna Transportation System (WNTS) is a critical subsea pipeline network in Indonesia that transports natural gas from the Natuna Sea. This region is known for its high-current velocity and complex seabed topology, making it prone to free span occurrences. Given these conditions, a detailed analysis of VIV effects under varying flow headings is essential for ensuring the reliability of the pipeline system.

This study addresses a key limitation found in previous research, such as [4, 5] which did not evaluate the influence of heading flow angles on pipeline fatigue. By simulating heading flow variations and calculating fatigue life



¹Department of Ocean Engineerig, Institut Teknologi Kalimantan, Balikpapan, 76127, Indonesia

²Naval Architecture Department, Institut Teknologi Kalimantan, Balikpapan, 76127, Indonesia

^{*}Corresponding Author | Luh Putri Adnyani | | luhputria@lecturer.itk.ac.id

using the Palmgren-Miner method and DNV-RP-F105 standards, this study provides a more comprehensive understanding of VIV-induced fatigue in free span subsea pipelines.

METHOD

Free-span modeling is a critical stage in analyzing flow behavior around subsea pipelines. This process involves creating a geometric representation of a pipeline section that is suspended above the seabed, where the pipe may be subject to vortex-induced vibrations (VIV). According to Zhou, et al. [12], accurate modeling must account for multiple parameters, including pipeline diameter, free-span length, and the characteristics of the surrounding flow field. In this study, to understand flow field around pipeline, numerical simulations has been undertaken using FLUENT. FLUENT software is an advanced commercial CFD code. It can simulate the flow filed of any case and shows good reliability. The flow past an artificial berm and a smooth circular cylinder has been simulated by solving numerically and 2D Navier-Stokes equations for unsteady, incompressible and turbulent flow. The governing equations for the flow around underwater pipeline are the continuity equation and the momentum equation [13].

$$\frac{\partial u_i}{\partial x_i} = 0 \tag{1}$$

$$\frac{\partial u_i}{\partial t} + u_j \frac{\partial u_i}{\partial x_j} = -\frac{1}{\rho} \frac{\partial p}{\partial x_i} + \frac{\partial (2\nu S_{ij} - \overline{u_i' u_j'})}{\partial x_j}$$
(2)

$$S_{ij} = \frac{1}{2} \left(\frac{\partial u_i}{\partial x_j} + \frac{\partial u_j}{\partial x_i} \right) \tag{3}$$

$$\overline{u_i'u_j'} = v_T \left(\frac{\partial u_i}{\partial x_j} + \frac{\partial u_j}{\partial x_i} \right) + \frac{2}{3} k \delta_{ij} \tag{4}$$

where u_i is the fluid velocity component in i direction, p is the pressure, ρ is the fluid density, v is the fluid kinetic viscosity, S_{ij} is the mean strain rate tensor, u_i' is the fluctuation of fluid velocity in i direction, $u_i'u_j'$ is the Reynolds stress tensor, v_T is the turbulence viscosity, and δ_{ij} is the Kronecker delta. Turbulence model $k - \omega$ is one of the most common model used to predict the effects of turbulence [14, 15].

As demonstrated by Zhang, et al. [16], Zhang, et al. [17], CFD-based simulation software enables detailed visualization and calculation of pressure distribution and flow velocity around the pipeline. The model was prepared with careful consideration of geometric factors, such as seabed profile and flow variations [18]. To support the analysis, the modeling was carried out using a two-dimensional (2D) approach. The 2D model provides an initial representation of the flow pattern around the pipeline and helps identify critical zones where vortex shedding is likely to occur.

The modeling process began with geometry generation in ANSYS DesignModeler. Boundary conditions and material properties were selected according to the guidelines provided in DNV-RP-F105 [19]. This methodology has been proven effective for identifying VIV phenomena and estimating pipeline fatigue life under free-span conditions [20]. The modeling procedure consisted of the following steps:

- a) Pipeline Geometry Identification The modeled pipeline geometry reflected actual field conditions, including free-span length, outer diameter, wall thickness, and any curvature radius. For this case study, geometry data were obtained from the WNTS Natuna project.
- b) Environmental Conditions Input parameters included water depth, seabed characteristics, and current velocity profiles. These data were used to define the hydrodynamic loading parameters in the simulation. Incorporating realistic environmental conditions ensured more accurate predictions of pipeline response to flow.
- c) Material Selection The pipeline material was chosen based on industry standards for subsea pipelines, such as specified grades of steel. Material properties, including Young's modulus, density, and Poisson's ratio, were defined in the model to influence the structural response of the pipeline during simulation.
- d) CFD Model Development A CAD model of the pipeline was generated in ANSYS DesignModeler, representing the free-span segment in accordance with field data. Relevant geometric details were incorporated to accurately replicate physical conditions.
- e) Application of Boundary Conditions Boundary conditions were applied to simulate pipeline constraints and flow domain limits. For example, both ends of the pipeline segment were assumed to be fixed to replicate in-situ restraint conditions during hydrodynamic loading.

- f) Meshing The meshing process subdivided the pipeline model into smaller finite elements to enable efficient numerical computation in CFD simulations. Mesh density was refined in the vicinity of the free-span region to capture detailed flow–structure interaction without excessive computational cost.
- g) Based on the free-span data, the gap between the pipeline and seabed can be estimated using a beam deflection approach, providing initial values for the span height to be used in subsequent VIV and fatigue life assessments.

$$\delta_{max} = \frac{5\omega l^4}{384EI} \tag{1}$$

Where δ_{max} is maximum deflection, ω is maximum submerged weight, l is span length, E is Modulus Young and I is moment inertia.

This research employed ANSYS Fluent 2025 R1 to simulate 2D flow across a subsea pipeline with a diameter of 0.6096 m and free span conditions. Simulations were conducted at heading flow angles of 30°, 45°, and 90° (see Figure 1) under varying Reynolds numbers (3.91×10⁵, 500, and 100) to capture both turbulent and transitional regimes. the mesh was structured and refined around the cylinder using inflation layers. boundary conditions included inlet velocity profiles derived from metocean data and outlet conditions based on pressure assumptions. The hydrodynamic force coefficients (cd and cl) and pressure distribution were extracted from simulations. Fatigue life was estimated using the Palmgren-Miner rule, applying stress range data into the S–N curve based on DNV-RP-F105. The cumulative fatigue damage and cycles were calculated to determine the fatigue life and critical locations across the span.

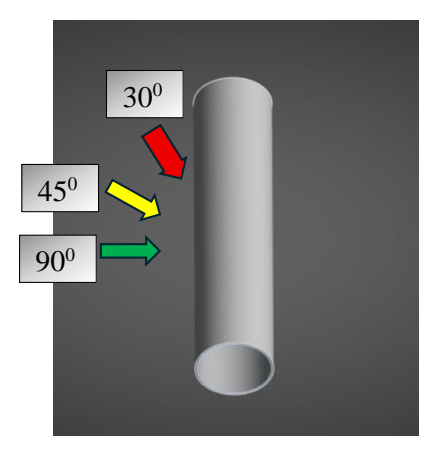


Figure 1. Heading Flow

Data collection

Pipe properties data used are shown in Table 1.

Tuble 17 1 repetites pipeline in 65 und 61 system							
Description	Value	Unit	Value	Unit			
Steel grade	API 5L – 65 PSL 2 QO/MO						
Pipeline route		Pempi	ng - WNTS				
Outside diameter (DO)	16	Inch	0,406	m			
Wall thickness	0,56	Inch	0,01422	m			
length	4	Km	4000	m			
Corrosion allowance	3	Mm	0,003	m			
Steel density	7850	Kg/m3	490,059	Lbs/ft ³			
Yong's modulus steel	207000	Mpa	30022811,7	Psi			
Design maximum pressure	14.89	Mpa	2160	Psi			
Service	GAS						
Fluid density max.(min)	5,30. (3,9)	Lbs/ft ³	84,90. (62,76)				

Table 1. Properties pipeline in US and SI system

Table 2. Current data						
		Unit				
Description	Design basis 1 years	Design basis 10 years	Design basis 100 years			
50% water depth	1.08	1.53	1.95	m/s		
100% water depth	1.01	1.43	1.82	m/s		
Maximum water depth		29		m		
Depth span		0.216		m		

Table 2. Current data

Table 3. Free span data for each condition

Pipeline load condition	Max.Allowable span length (m)	Governing criteria
Instalation	17. 36	In-line (single span)
Hydrotest	17.98	In-line (multi span)
Operation uncorrroded	11.67	In-line (single span)
Operation corroded	9.62	In-line (single span)

RESULTS AND DISCUSSION

Simulation results show that flow patterns and pressure contours vary significantly with heading angle. At 90° , clear vortex shedding occurred symmetrically around the pipe, resulting in high fluctuating lift forces. C_d and C_l values peaked at this orientation, particularly at maximum and minimum span depths. At 30° and 45° , flow separation became asymmetric, generating alternating wake structures. The drag coefficient (C_d) decreased while the lift coefficient (C_l) remained oscillatory.

The fatigue life calculation for a subsea pipeline in a free-span condition is focused on the influence of lift forces generated by the Vortex-Induced Vibration (VIV) phenomenon. As previously discussed, the lift force acting periodically on the pipeline induces transverse vibrations that fluctuate over time. These fluctuations produce dynamic bending moments, which are a primary cause of cyclic stresses within the pipeline structure. The first step in estimating fatigue life involves determining the maximum bending moment amplitude resulting from the pipeline's response to the lift force. This moment value is then used to calculate the cyclic bending stress occurring on the pipeline cross-section.

The bending moment arises from the lift force acting on the surface of a cylindrical object when subjected to fluid flow. This force, when multiplied by the span length, produces a bending moment that serves as an initial indicator of the fluid load's effect on the structure. The resulting bending moment is subsequently used to determine the bending stress within the structure. This stress reflects the distribution of internal loads experienced by the material due to bending and serves as a critical parameter in assessing the structural safety and stiffness. The analysis was conducted for three angles of attack—90°, 45°, and 30°—and for three depth span conditions (maximum, average, and minimum). The lift force values employed in the analysis were derived from simulation results for each condition, using either maximum or average values depending on the analytical requirements.

$$M = L x F l (2)$$

Where M is the maximum bending moment, L is pipe span length, and Fl is the maximum lift force due to VIV. The obtained bending moment values are subsequently used to calculate the bending stress experienced by the pipeline. The bending stress (σ) is calculated using the following equation:

$$\sigma = \frac{M \times D}{2 \times I} \tag{3}$$

Where σ is the maximum bending stress, M is the maximum bending moment, D is the outside diameter, and I is moment inertia.

This irregularity translates into lower but still notable fatigue damage. Fatigue analysis reveals that the 90° heading flow caused the most severe fatigue due to higher oscillatory forces, reducing fatigue life to below 10^{5} cycles. In contrast, 30° showed longer life spans. The fatigue life distribution along the span indicates that maximum stress occurred at mid-span in the 90° case due to amplified oscillation.

Heading (°)	Depth Span	Lift Force Cd	Span	Bending	Bending
		(N)	Length (m)	Moment (Nm)	Stress (Pa)
90	Maximum	190.7	44.57	8499.9	5131638.5
	Mean	274.6	44.57	12240.7	7390026.5
30	Maximum	-54.9	44.57	-2449.1	1478485.6
	Mean	-127.9	44.57	-5702.3	3442648.9
45	Maximum	95.2	44.57	4245.3	2563001.4
	Mean	107.8	44.57	4805.2	2901037.9

Table 4. Bending Moment and Bending Stress

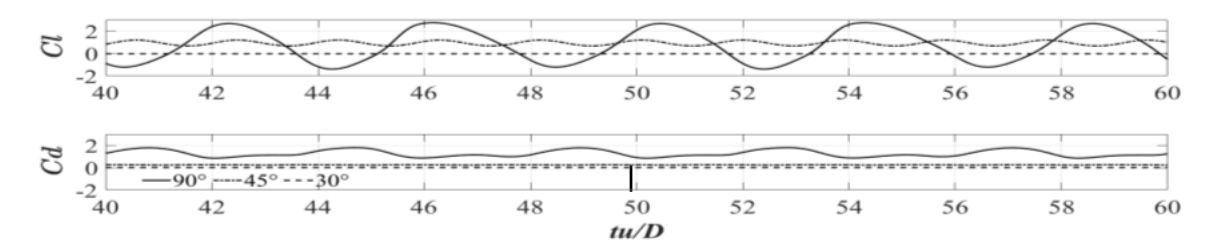


Figure 2. Lift and drag coefficient under variation of heading flow

Based on the lift force as shown in Table 4, lift coefficient can be calculated using the following equation:

$$F_L = \frac{1}{2} \rho U^2. C_L A \sin \sin(\theta)$$
 (4)

With ρ is fluid density, U is fluid velocity, A is surface area for pipe projection, C_L is the drag coefficient, and θ is the heading flow angle. From the previous results in this study, C_D and C_L can also be calculated using CFD as shown in Figure 2.

This study evaluates time histories of lift and drag coefficients in Figure 2 (Cl and Cd versus non-dimensional time tu/D for heading angles 30°, 45°, and 90°) that show that the cross-flow response is strongly heading-dependent: the 90° case exhibits nearly sinusoidal Cl oscillations with the largest amplitude, the 45° case shows a weaker but still periodic response, and the 30° case is only mildly excited. In contrast, Cd fluctuations remain small around a mean value for all headings, indicating that fatigue is predominantly controlled by the lift component.

This pattern is consistent with towing-tank experiments on multi-span pipelines by Xu, et al. [5], who observed that when the flow is approximately normal to the pipeline axis the cross-flow response becomes strongly periodic, with clear lock-in and dominant lift-induced vibrations, whereas oblique incidence substantially reduces the vibration amplitude and modifies the wake symmetry. In their tests, the largest response occurs under near-normal flow and decays rapidly as the yaw angle increases—exactly the qualitative trend seen in Cl signals for 90°, 45°, and 30° in this study. Experimental investigations on pipelines near the seabed also show that oblique flow leads to asymmetric vortex shedding and reduced cross-flow amplitudes compared with normal incidence, particularly at yaw angles around 30°, which again supports the simulated heading-angle sensitivity [21].

In terms of coefficient value, classical experiments on free-span and near-bed pipelines generally report peak lift coefficients in the range $|CI| \approx 0.5$ –1.1 during lock-in, with drag coefficients around $Cd \approx 0.9$ –1.4 depending on Reynolds number and proximity to the seabed [22]. Figure 2 indicate that the simulated Cl for the 90° case reaches values of order O(1), while Cd oscillations remain comparatively small and slowly varying, placing the CFD results within the broad experimental envelope for VIV-dominated flow. Similar behaviour—strongly oscillatory lift with modest drag variation—has been reported in detailed flume tests on long free spans near the seabed and in oblique shear flows, where the lift coefficient carries most of the fatigue-relevant energy while drag contributes primarily to mean loading.

This study concludes that the 90° heading produces the largest bending stresses and the shortest fatigue life, while 30° and 45° headings yield much longer lives, often by several orders of magnitude, because the Cl oscillations are significantly attenuated. This directional dependence aligns with recent very-high-cycle fatigue tests on free-spanning pipelines, which demonstrate that lock-in under strong cross-flow excitation can reduce fatigue life to the order of 10^{5} – 10^{7} cycles, whereas off-design conditions with weaker VIV produce lives extending into the very-high-cycle regime [4]. Field-oriented fatigue assessments on pipelines in sand-wave regions similarly identify VIV as the

dominant driver of damage and emphasize that only a subset of span orientations and hydrodynamic conditions produce critical fatigue hot-spots [23].

Calculating Fatigue Life

Table 5. Safety factor for fatigue [19]

	Safety Class				
Safety Factor	Low	Normal	High		
η	1.0	0.5	0.25		
yk	1.0	1.15	1.30		
ys		1.3			
Y on, IL		1.1			
Y on, IL		1.2			

Table 6. Cycle & Damage accumulation 90⁰

	Heading 90° maximum				Heading 90° mean		
Time	Bending	N	DFAT	Bending	N	DFAT	
Step	stress			stress			
1	5.08E+08	711.7197437	0.001405	5.59E+08	5.35E+02	0.001868	
2	5.13E+06	690608346.9	1.45E-09	7.11E+06	2.60E+08	3.85E-09	
3	3.24E+06	2741369841	3.65E-10	3.15E+06	2.99E+09	3.34E-10	
4	2.68E+05	4.85354E+12	2.06E-13	1.64E+07	2.11E+07	4.73E-08	
5	5.27E+06	637649705.8	1.57E-09	2.71E+07	4.67E+06	2.14E-07	
6	1.12E+07	66847634.71	1.5E-08	3.30E+07	2.60E+06	3.84E-07	
7	1.68E+07	19665369.06	5.09E-08	3.45E+07	2.28E+06	4.38E-07	
8	2.15E+07	9410957.292	1.06E-07	3.36E+07	2.45E+06	4.08E-07	
9	2.47E+07	6179236.511	1.62E-07	3.22E+07	2.79E+06	3.59E-07	
10	2.66E+07	4965368.36	2.01E-07	3.12E+07	3.08E+06	3.25E-07	
11	2.71E+07	4667211.336	2.14E-07	3.05E+07	3.29E+06	3.04E-07	
12	2.71E+07	4674573.251	2.14E-07	2.97E+07	3.55E+06	2.82E-07	
13	2.68E+07	4830194.965	2.07E-07	2.89E+07	3.85E+06	2.6E-07	
14	2.62E+07	5206221.654	1.92E-07	2.81E+07	4.19E+06	2.39E-07	

The S-N curve (Stress vs. Number of Cycles) is used to illustrate the relationship between cyclic stress (S) and the number of cycles to failure (N) in a material subjected to fatigue loading. This curve is typically presented on a logarithmic scale to facilitate the interpretation of the exponential relationship between stress magnitude and the number of cycles to failure. From the stress range obtained using the appropriate material S-N curve, the N cycle value is obtained for the basis of fatigue calculation.

$$N_i = \frac{A}{\sigma^3} \tag{5}$$

Heading 45° maximum				Heading 45° mean			
Time	Bending stress	N	DFAT	Bending	N	DFAT	
Step				stress			
1	308674474.9	3.17E+03	3.15E-04	3.36E+08	2.45E+03	4.07E-04	
2	2563001.436	5.54E+09	1.80E-10	2.90E+06	3.82E+09	2.62E-10	
3	105492.7688	7.95E+13	1.26E-14	3.57E+05	2.05E+12	4.89E-13	
4	1276023.262	4.49E+10	2.23E-11	5.65E+06	5.19E+08	1.93E-09	
5	3307940.608	2.58E+09	3.88E-10	1.18E+07	5.64E+07	1.77E-08	
6	5878113.515	4.60E+08	2.18E-09	1.70E+07	1.89E+07	5.29E-08	
7	8548728.437	1.49E+08	6.69E-09	2.03E+07	1.12E+07	8.96E-08	
8	11231003.93	6.59E+07	1.52E-08	2.15E+07	9.39E+06	1.06E-07	
9	13808394.93	3.54E+07	2.82E-08	2.13E+07	9.62E+06	1.04E-07	
10	15320048.42	2.60E+07	3.85E-08	2.07E+07	1.05E+07	9.51E-08	
11	16353792.6	2.13E+07	4.69E-08	1.99E+07	1.19E+07	8.43E-08	
12	16454588.94	2.09E+07	4.77E-08	1.89E+07	1.39E+07	7.22E-08	
13	15813509.82	2.36E+07	4.24E-08	1.77E+07	1.68E+07	5.97E-08	
14	14932461.42	2.80E+07	3.57E-08	1.65E+07	2.09E+07	4.78E-08	

Table 7. Cycle & Damage accumulation 45⁰

Where A is 1010.97, m is 3, and σ is cyclic stress (Mpa). From Equation 4, the number of cycles to failure N_{cycle} can be determined based on the stress range experienced by the material. This relationship indicates that the higher the applied stress, the fewer cycles are required for fatigue failure to occur. This model forms the basis for fatigue life estimation of the pipeline in this study, particularly in the context of vibrations induced by vortex shedding around a free-span pipeline.

$$D = \sum_{i=0}^{m} \frac{n_i}{N_i} \tag{6}$$

Where D is total accumulated fatigue damage (fatigue damage index). The structure is considered to have failed if $D \ge 1$; n_i is actual number of cycles at the i^{th} stress level; N_i is the maximum number of cycles that the material can withstand at the i^{th} stress level, based on the S-N (stress-life) curve. The fatigue life of the pipeline is calculated using the following equation:

$$T_f = \frac{T_{exp}}{DFAT.\mu} \tag{7}$$

Where T_{exp} is estimated lifetime, *DFAT* is fatigue damage factor, and μ is safety factor for fatigue. The fatigue safety factor used in the calculation of stress range and the determination of the operational life of subsea pipelines is shown in Table 5, adapted from *DNV-RP-F105* [19].

The bending moment arises from the lift force acting on the surface of an elliptical object when subjected to fluid flow. This force, when multiplied by the span length, produces a bending moment that serves as an initial indicator of the influence of fluid loading on the structure. The resulting bending moment is then used to determine the bending stress within the structure. This stress represents the distribution of internal loads experienced by the material due to bending and serves as a key parameter in evaluating the structural safety and stiffness. The analysis was carried out for three angles of attack—90°, 45°, and 30°—and under three depth-span conditions (maximum, average, and minimum). The lift force values used in the analysis were derived from simulation results for each condition, employing either maximum or average values depending on the analytical requirements.

Table 6 presents the cycle and damage accumulation analysis for the 90° heading condition under both maximum and mean bending stress scenarios. For the maximum bending stress case, values range from $5.08 \times 10^8\,$ to $2.62 \times 10^7\,$ Pa, corresponding to fatigue life cycles (N) from 711.72 to 4.85×10^{12} , with associated damage factors (DFAT) between $2.06 \times 10^{-13}\,$ and 0.001405. In the mean bending stress scenario, the stress ranges from $5.59 \times 10^8\,$ to $2.81 \times 10^7\,$ Pa, with N values from $535.00\,$ to $2.11 \times 10^7\,$, and DFAT ranging from $2.39 \times 10^{-7}\,$ to 0.001868. The results indicate that higher bending stresses produce significantly fewer cycles to failure and larger damage accumulation, highlighting the sensitivity of fatigue damage to stress magnitude. These findings underscore the importance of accurately estimating bending stresses in free-span pipeline assessments to predict service life and ensure structural safety.

Table 7 summarizes the cycle and damage accumulation results for the 45° heading condition under both maximum and mean bending stress scenarios. For the maximum bending stress case, values range from 3.09 \times 108 to 1.49 \times 107 Pa, with corresponding fatigue life cycles (N) from 3.17 \times 103 to 7.95 \times 1013, and damage factors (DFAT) between 1.26 \times 107 and 3.88 \times 107 and 3.88 \times 107 and 9.39 \times 106 , and DFAT from 1.93 \times 107 to 7.22 \times 107 to 7.22 \times 107 These results indicate that higher bending stresses significantly reduce the number of cycles to failure and increase damage accumulation, emphasizing the influence of stress magnitude and heading angle on fatigue performance. This analysis highlights the necessity of precise bending stress evaluation for accurate fatigue life prediction in subsea pipeline freespan conditions.

		,	C			
	Heading 30° m	naximum	Headi	ng 30° mear	ı	
Time Step	Bending stress	N	DFAT	Bending stress	N	DFAT
1	20637733.5	1.06E+07	9.42E-08	2.13E+07	9.71E+06	1.03E-07
2	5695138.816	5.05E+08	1.98E-09	5.08E+06	7.13E+08	1.40E-09
3	5260983.468	6.41E+08	1.56E-09	5.17E+06	6.74E+08	1.48E-09
4	4885898.387	8.00E+08	1.25E-09	5.10E+06	7.06E+08	1.42E-09
5	4581986.569	9.70E+08	1.03E-09	5.04E+06	7.27E+08	1.38E-09
6	4338566.703	1.14E+09	8.75E-10	5.01E+06	7.43E+08	1.35E-09
7	4137083.472	1.32E+09	7.59E-10	4.98E+06	7.55E+08	1.32E-09
8	3968903.4	1.49E+09	6.70E-10	4.97E+06	7.60E+08	1.32E-09
9	3827841.69	1.66E+09	6.01E-10	4.92E+06	7.81E+08	1.28E-09
10	3707199.117	1.83E+09	5.46E-10	4.87E+06	8.09E+08	1.24E-09
11	3603804.967	1.99E+09	5.02E-10	4.82E+06	8.34E+08	1.20E-09
12	3513716.925	2.15E+09	4.65E-10	4.77E+06	8.60E+08	1.16E-09
13	3434656.822	2.30E+09	4.34E-10	4.72E+06	8.88E+08	1.13E-09
14	3365256.854	2.45E+09	4.08E-10	4.67E+06	9.14E+08	1.09E-09

Table 8. Cycle & Damage accumulation 30⁰

Table 9. Mean of fatigue life

Heading (°)	Depth Span Condition	Re100	Re500	Re 3.91×10 ⁵		
Treating ()		(Tahun)				
00	Maximum	7.89×10^{13}	5.36×10^9	3.61×10^{17}		
90	Mean Maximum		$\substack{2.45 \times 10^8 \\ 2.54 \times 10^{13}}$			
30	Mean Maximum		$\substack{4.18 \times 10^{12} \\ 1.62 \times 10^{10}}$			
45	Mean	2.24×10^{16}	1.75×10^9	4.75×10^{10}		

Table 8 presents the cycle and damage accumulation results for the 30° heading condition under both maximum and mean bending stress scenarios. For the maximum bending stress case, values range from $3.36\times10^6\,$ to $2.06\times10^7\,$ Pa, with corresponding fatigue life cycles (N) between $1.06\times10^7\,$ and $2.45\times10^9\,$, and damage factors (DFAT) from $9.42\times10^{-8}\,$ to $4.08\times10^{-10}\,$. In the mean bending stress case, stresses range from $4.67\times10^6\,$ to $2.13\times10^7\,$ Pa, with N values from $6.74\times10^8\,$ to $9.71\times10^6\,$, and DFAT between $1.03\times10^{-7}\,$ and $1.09\times10^{-9}\,$. The data indicate that higher bending stresses lead to fewer cycles to failure and increased damage accumulation, even at a lower heading angle, highlighting the sensitivity of fatigue performance to bending stress magnitude and operational orientation of the pipeline.

Average fatigue life values of subsea pipelines based on flow angle variations $(30^{\circ}, 45^{\circ}, \text{ and } 90^{\circ})$, and three Reynolds number conditions (Re = 100, 500, and 3.91×10^{5}) representing laminar to turbulent flow. Results show that fatigue life is strongly influenced by fluid flow characteristics, where higher flow velocities (Re = 3.91×10^{5}) result in generally lower fatigue life values compared to smaller Re. This occurs because the higher the Reynolds number, the greater the dynamic forces acting on the pipe surface, especially due to the vortex-induced vibration (VIV) phenomenon, thereby increasing the amplitude of oscillations and cyclic stresses that accelerate fatigue damage.

However, overall, the fatigue life values obtained are very high. This can be explained by the simulation approach used, where the calculation only considers the lift force through the CL coefficient as the dominant excitation in the cross-flow direction. Meanwhile, contributions from drag force (CD), axial load (in-line), pipe internal pressure, as well as complex effects from interaction with real sea conditions have not been incorporated into the model. Therefore, although the simulation results provide a conservative estimate, the displayed fatigue life values still do not fully reflect the extreme conditions in the field.

CONCLUSION

Overall, this study consistent with the main experimental findings on subsea pipeline VIV. The analysis confirms that heading flow angle is a critical factor in determining subsea pipeline fatigue performance under free-span conditions. Across all Reynolds numbers, pipelines oriented at 90° to the main current experienced the highest oscillatory lift forces, leading to maximum bending stresses of up to 5.59×10^8 Pa and the shortest fatigue life. In contrast, oblique orientations (30°–45°) reduced vortex shedding intensity, cyclic stress amplitudes, and cumulative damage by more than two orders of magnitude in some cases. For the WNTS pipeline, maintaining an oblique alignment could increase fatigue life from less than 10^5 cycles at 90° to more than 10^{16} cycles at 30° under low-Reynolds conditions, significantly lowering the likelihood of premature failure. However, the simulated fatigue life values are conservative estimates, as the model considered only cross-flow lift forces (Cl) without accounting for drag, in-line forces, internal pressure, or seabed—pipeline interaction. Future studies should integrate these additional load components and validate results with field measurements to ensure comprehensive risk assessment. The outcomes of this research provide actionable guidance for subsea pipeline design, installation planning, and integrity management in high-current offshore environments.

REFERENCES

- [1] N. Hadi, M. Helmi, E. Cathaputra, D. Priadi, and D. Dhaneswara, "Freespan Analysis for Subsea Pipeline Integrity Management Strategy," *Journal of Materials Exploration and Findings (JMEF)*, vol. 1, no. 3, p. 5, 2023.
- [2] M. Mohaddes Pour and S. S. Razavi Taheri, "Free Span Analysis for Submarine Pipelines," *Shock and Vibration*, vol. 2021, no. 1, p. 9305129, 2021. doi: 10.1155/2021/9305129
- [3] A. A. Shittu, F. Kara, A. Aliyu, and O. Unaeze, "Review of pipeline span analysis," *World Journal of Engineering*, vol. 16, no. 1, pp. 166-190, 2019. https://doi.org/10.1108/WJE-09-2017-0296
- [4] Q. Song, J. Liu, and F. Gao, "Very High Cycle Fatigue Life of Free-Spanning Subsea Pipeline Subjected to Vortex-Induced Vibrations," *Journal of Marine Science and Engineering*, vol. 12, no. 9, p. 1556, 2024. https://doi.org/10.3390/jmse12091556
- [5] W.-h. Xu, K. Jia, Y.-x. Ma, and Z.-y. Song, "Vortex-induced vibration response features of a submarine multi-span pipeline via towing tank experimental tests," *China Ocean Engineering*, vol. 37, no. 2, pp. 175-189, 2023. doi: 10.1007/s13344-023-0016-4

- [6] D. Priyanta and A. Abdullah, "Analysis of the Suppression Device as Vortex Induced Vibration (VIV) Reducer on Free Span using Finite Element Method," *International Journal of Marine Engineering Innovation and Research*, vol. 1, 12/01 2016, doi: 10.12962/j25481479.v1i1.1387.
- [7] S. A. Shittu, *Numerical Simulation of Vortex-induced Vibration of Free Spanning Underwater Pipeline Close to the Seabed.* The University of Manchester (United Kingdom), 2022.
- [8] F. Xiao and H.-C. Chen, "CFD simulation of vortex-induced vibrations of free span pipelines including pipe-soil interactions," in *ISOPE International Ocean and Polar Engineering Conference*, 2015: ISOPE, pp. ISOPE-I-15-267.
- [9] B. M. Bossio V, A. J. Blanco A, and E. L. Casanova M, "Numerical modeling of the dynamical interaction between slug flow and vortex induced vibration in horizontal submarine pipelines," *Journal of Offshore Mechanics and Arctic Engineering*, vol. 136, no. 4, p. 041803, 2014. https://doi.org/10.1115/1.4028027
- [10] A. Ragab, W. Brandstaetter, and S. Shalaby, "CFD-simulation of multiphase flows in horizontal and inclined pipelines," *Oil, Gas (Hamburg)*, vol. 34, 2008.
- [11] R. H. Willden and J. M. R. Graham, "CFD simulations of the vortex-induced vibrations of model riser pipes," in *International Conference on Offshore Mechanics and Arctic Engineering*, 2005, vol. 41979, pp. 837-846.
- [12] J. Zhou, X. Li, and R. Dong, "Experimental study and numerical analysis on free spanning submarine pipeline under dynamic excitation," in *ISOPE International Ocean and Polar Engineering Conference*, 2005: ISOPE, pp. ISOPE-I-05-139.
- [13] Z. Zhang, B. Shi, Y. Guo, and L. Yang, "Numerical investigation on critical length of impermeable plate below underwater pipeline under steady current," *Science China Technological Sciences*, vol. 56, pp. 1232-1240, 2013.
- [14] L. Dongfang and C. Liang, "Numerical modeling of flow and scour below a pipeline in currents, Part I: Flow simulation," *Coastal Engineering*, vol. 52, pp. 25-42, 2004.
- [15] H. An, L. Cheng, and M. Zhao, "Numerical simulation of a partially buried pipeline in a permeable seabed subject to combined oscillatory flow and steady current," *Ocean engineering*, vol. 38, no. 10, pp. 1225-1236, 2011. https://doi.org/10.1016/j.oceaneng.2011.05.010
- [16] B. Zhang, H. An, S. Draper, H. Jiang, L. Cheng, and X. Zhao, "Three-Dimensional Flow Around a Span Shoulder of a Pipeline/Cable: Insight From Experiments Combined With Numerical Modelling," in *International Conference on Offshore Mechanics and Arctic Engineering*, 2024, vol. 87844: American Society of Mechanical Engineers, p. V006T08A023.
- [17] B. Zhang, H. An, S. Draper, H. Jiang, and L. Cheng, "Numerical Simulations of Three-Dimensional Scour Below Subsea Pipelines/Cables Under Steady Current Conditions," in *International Conference on Offshore Mechanics and Arctic Engineering*, 2023, vol. 86892: American Society of Mechanical Engineers, p. V007T08A030. https://doi.org/10.1115/OMAE2023-104579
- [18] J. Fredsøe, "Pipeline–Seabed Interaction," (in En), *Journal of Waterway, Port, Coastal, and Ocean Engineering*, vol. 142, no. 6, p. 03116002, 2016/11/01/ 2016, doi: 10.1061/(ASCE)WW.1943-5460.0000352.
- [19] DNV, "Free spanning pipelines," *Recommended practice DNV-RPF105*, pp. 1-46, 2006.
- [20] J. Wang, F. Steven Wang, G. Duan, and P. Jukes, "VIV analysis of pipelines under complex span conditions," *Journal of Marine Science and Application*, vol. 8, no. 2, pp. 105-109, 2009.
- [21] H. Zhu, H. Zhao, and N. Srinil, "Experimental investigation on vortex-induced vibration and solid-structure impact of a near-bottom horizontal flexible pipeline in oblique shear flow," *Journal of*

- *Fluids and Structures*, vol. 106, p. 103356, 2021/10/01/ 2021, doi: https://doi.org/10.1016/j.jfluidstructs.2021.103356.
- [22] X. Li, Y. Wang, G. Li, M. Jiang, and X. He, "Experimental investigation of vortex-induced vibrations of long free spans near seabed," *Science China Technological Sciences*, vol. 54, no. 3, pp. 698-704, 2011/03/01 2011, doi: 10.1007/s11431-010-4258-z.
- [23] X. Zou, B. Xie, Z. Zang, E. Chen, and J. Hou, "Vortex-Induced Vibration and Fatigue Damage Assessment for a Submarine Pipeline on a Sand Wave Seabed," *Journal of Marine Science and Engineering*, vol. 11, no. 10, p. 2031, 2023. [Online]. Available: https://www.mdpi.com/2077-1312/11/10/2031.